

Molecular Dynamics by Light Scattering in the Condensed Phases of Ar, Kr, and Xe

P. A. Fleury, J. M. Worlock, and H. L. Carter

Bell Telephone Laboratories, Murray Hill, New Jersey 07974

(Received 26 January 1973)

Temperature dependence of molecular dynamics as revealed by intermolecular and second-order Raman scattering in the condensed rare gases are reported with special emphasis on the behavior near the melting transition.

Inelastic light scattering from higher-order phonon or intermolecular processes is capable in principle of providing detailed information on the short-time dynamics of both the solid and the liquid states. Unfortunately, second-order (or two-phonon) Raman spectra have proven extremely difficult to interpret even in solids as simple as the alkali halides.¹ Similarly, the closely related phenomenon of intermolecular light scattering recently observed in liquids remains to be fully understood.² The materials which offer the greatest hope for elucidating these two phenomena are the condensed phases of the classical rare gases. We report here inelastic light scattering measurements of the spectral line shapes, strengths, and polarization properties for both the solid and liquid phases of Ar, Kr, and Xe. Our results represent the first direct confirmation that the dynamic processes occurring over the entire frequency range, which includes even the characteristic inverse collision time (10^{+12} – 10^{+13} sec⁻¹), scale in simple fluids according to an extension of the corresponding-states principle³ (CSP). Further, our comparisons of the liquid/solid spectra show the high-frequency dynamics to be virtually unaffected by the melting transition. In addition, we report the first observation of the second-order Raman effect in these solids, and find that the low-temperature results agree quite well with theoretical lattice dynamic calculations⁴ provided that zone-boundary phonon frequencies for the different materials are scaled according to the dynamic CSP. Finally, the absolute scattering efficiencies we have measured imply that the relative contributions of electronic and atomic configurational processes to nonlinear optic coefficients are quite different in the liquid and solid states.

The spectra (obtained at 90° scattering angle) were excited with 200 mW of linearly polarized 5145- or 4880-Å argon-ion laser light. All scattering efficiencies quoted in this paper are appropriate to 4880 Å excitation. The sample gases were condensed directly into a specially de-

signed ($1 \times 1 \times 2$ cm³) temperature-controlled ($\pm 0.02^\circ\text{K}$) cell. Using vertically distributed heaters on the cell walls to obtain the required temperature gradients, the solid was then grown slowly (~ 0.5 mm/h) from the cell base. Before cooling well below T_m , the solid was sublimed away from the cell walls in order to avoid deterioration of optical quality caused by differential thermal contraction. The sample was then cooled by lowering the base temperature while continually adjusting the ambient gas pressure to slightly above the solid's vapor pressure corresponding to the base temperature.⁵ Crystals of acceptable optical quality were thus obtained down to temperatures of $\sim 15^\circ\text{K}$. All scattered intensities were measured relative to the integrated intensity of the 992-cm⁻¹ vibrational line of liquid benzene at room temperature, whose absolute value is known.⁶

Figure 1 shows that the liquid intermolecular spectra of all three materials are adequately described by the function² $h(\omega) = h_0 \exp(-\omega/\Delta)$, so that when expressed in terms of a properly scaled dimensionless frequency, the spectral shapes fall on a universal curve. This behavior extends the familiar CSP (which states that thermodynamic and transport coefficients for systems with the same form of intermolecular potential should scale directly with the parameters of that potential) to high-frequency dynamics. Our previous empirical expression for Δ , which accurately describes the ρ and T dependence over large ranges, can be written in the following form:

$$\Delta(\rho, T) = \frac{A}{2\pi c} \left(\frac{\epsilon}{M\sigma^2} \right)^{1/2} \left(\frac{kT}{\epsilon} \right)^{1/2} \left[1 + \left(\frac{B\sigma^3}{M} \rho \right)^2 \right], \quad (1)$$

which clearly illustrates its CSP nature. Here c is the speed of light (so that Δ has units of cm⁻¹); M , σ , and ϵ are the atomic mass, Lennard-Jones distance, and energy parameters, respectively. A and B are dimensionless parameters whose values of 3.0 ± 0.1 and 2.0 ± 0.1 , respectively, produce excellent agreement with our observa-

tions covering $0.7 < kT/\epsilon < 4$ and $0.05 < \rho\sigma^3/M < 1$. Numerical evaluations of Eq. (1) for the liquids at their triple points predict Δ_{TP} 's of 22.1, 16.7,

and 14.4 cm^{-1} for Ar, Kr, and Xe, respectively, using 3.0 for A and 2.0 for B . These are in excellent agreement with the experimental values of 24, 17, and 14 cm^{-1} , respectively, obtained from Fig. 1.

The observed spectra in the solids just below T_m , also shown in Fig. 1, indicate that the high-frequency dynamics ($\omega > \omega_D$, the zero-temperature Debye frequency) in these simple materials undergo negligible change at the melting transition. Although it is natural to attribute the solid spectra to second-order (or two-phonon) Raman scattering, the spectra in Fig. 1 show none of the structure expected from lattice dynamical calculations of well-defined phonon modes in an fcc lattice.⁴ To establish the connection between the spectra of Fig. 1 and the second-order Raman calculations, we have studied the temperature dependence of the solid spectra down to $\sim 0.1T_m$ in both Kr and Xe. Figure 2 shows some results in Xe.

The general trends exhibited by these spectra as T is decreased are (1) a decrease in the high-frequency tail and a sharpening of the high-frequency cutoff (in good agreement with the calculated value of 88 cm^{-1}); (2) the emergence of the $2TA(0.5, 0.5, 0.5)$ peak at higher temperature than the LA-TA or $2LA$ peaks; and (3) the semi-quantitative agreement of the low-temperature shape with that calculated by theory. We note that the positions of the features including the cutoff indicated in Fig. 2(c) were obtained by scaling, according to the CSP, the frequencies calculated by Werthamer, Gray, and Koehler for Ar.⁴ The behavior observed in solid Kr is quite similar. There the observed cutoff is within 1% of the predicted 104-cm^{-1} value.

Utilizing the measured integrated intensity for the 992-cm^{-1} line in benzene⁶ ($h_T = 2.24 \times 10^{-7} \text{ cm}^{-1} \text{ sr}^{-1}$), we find integrated Stokes intensities of 0.18×10^{-8} , 0.83×10^{-8} , and $2.76 \times 10^{-8} \text{ cm}^{-1} \text{ sr}^{-1}$ for Ar, Kr, and Xe liquids, respectively. The values of h_0 , in terms of which Fig. 1 is calibrated, are 0.75×10^{-10} , 4.8×10^{-10} , and $19.7 \times 10^{-10} \text{ cm}^{-1} \text{ sr}^{-1}/\text{cm}^{-1}$ for Ar, Kr, and Xe, respectively, where $h_T = h_0 \Delta$ follows from the exponential spectral shape. Note that the solid spectra are considerably weaker in each case, in marked contrast to the previously observed situation⁸ in both He^3 and He^4 . The ratios of liquid-to-solid integrated intensities are 4.2, 9.4, and 8.9, for Ar, Kr, and Xe, respectively. Note that essentially *all* of the decrease upon entering the solid phases occurs in the low-frequency

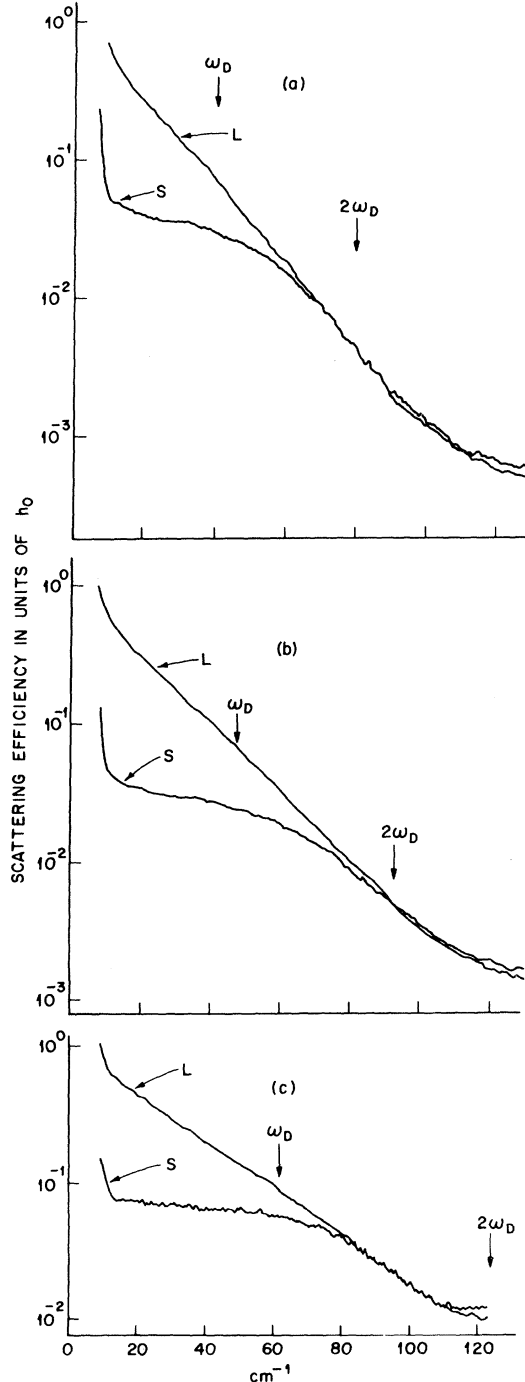


FIG. 1. Depolarized inelastic light-scattering spectra for the liquid (L) and solid (S) phases of (a) Xe, (b) Kr, and (c) Ar. Note the logarithmic intensity scale. Saturation in falloff above 120 cm^{-1} is due to background fluorescence from cell walls.

spectral regions.

While no adequate theory exists for the intensity of the intermolecular scattering in the liquid

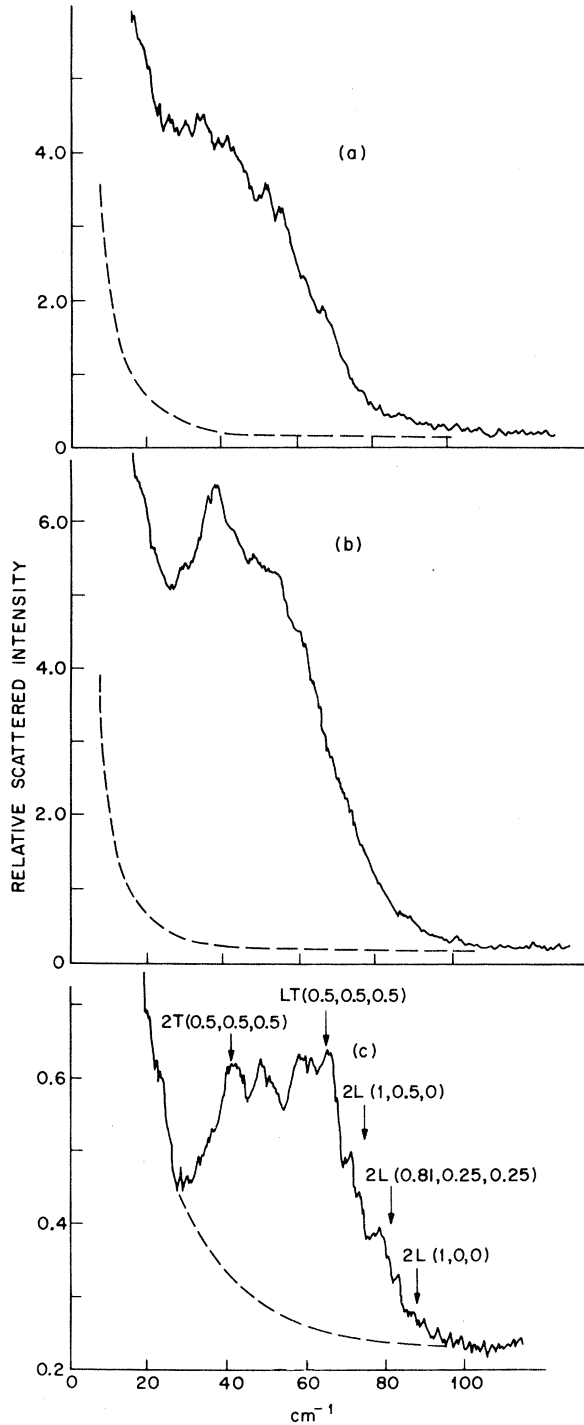


FIG. 2. Depolarized second-order Raman spectrum in solid Xe at (a) 145°K, (b) 116°K, and (c) 30°K. Arrows in (c) indicate positions of zone-boundary longitudinal (*L*) and transverse (*T*) features scaled by the CSP from Ar calculations of Ref. 4.

phases, specific predictions have been made for the second-order Raman spectra of the solid rare gases.⁴ These can be approximated to account for finite temperature, refractive index (η), and lattice sum effects by⁹

$$h_T = \frac{N}{V} \left(\frac{\alpha_0}{a^3} \right)^4 \left(\frac{\omega_i}{c} \right)^4 a^6 \left(\frac{\hbar}{M\omega_D a^2} \right)^2 Z^2 \times \left(\frac{\eta^2 + 2}{3} \right)^2 f \left(\frac{\hbar\omega_D}{kT} \right), \quad (2)$$

where α_0 is the atomic polarizability, a the lattice parameter, Z the number of nearest neighbors, and ω_i the laser frequency; $f(x) = (1 - e^{-x})^{-2}$. The calculated values of h_T are 4.6×10^{-10} , 6.9×10^{-10} , and $21.4 \times 10^{-10} \text{ cm}^{-1} \text{ sr}^{-1}$ for Ar, Kr, and Xe, respectively. The corresponding experimental values are 4.6×10^{-10} , 9.4×10^{-10} , and $33.6 \times 10^{-10} \text{ cm}^{-1} \text{ sr}^{-1}$. The agreement is quite good; but should not be considered quantitative to better than a factor of 2 because of experimental uncertainties and the approximations leading to Eq. (2). We note that the integrated intensity in solid helium is about $\frac{1}{10}$ that in solid argon.⁸

For all liquids and for the solids just below T_m the spectral shapes exhibited no discernible polarization dependence. In all these cases the depolarization ratio was measured as 0.75 ± 0.05 . For the solids at lower temperatures, the emergence of identifiable two-phonon structure was associated with definite polarization dependence of the spectral shapes, suggesting that our samples were predominantly single crystals.

The integrated intensity of the intermolecular light scattering can be simply related to the nonlinear optical susceptibility¹⁰ tensor which among other things governs self-trapping (the optical Kerr effect) and self-phase modulation of light.¹¹ The microscopic mechanism of the Kerr coefficient in condensed media has been the object of considerable interest,¹⁰ and calculations have been carried out to assess the relative importance of the so-called "electronic" and "atomic configurational" mechanisms.¹⁰ Our measurements of absolute intensities in the ordered (solid) and disordered (liquid) states of three simple materials should provide a means of testing these various microscopic theories of nonlinear optical coefficients.

In summary, we have shown that, first, the rare-gas liquids and solids obey in detail the dynamic statement of the correspondence-states principle over a continuous frequency range up to at least the atomic collision frequency. Sec-

ond, the short-time dynamics of all the simple fluids over remarkably large ranges of density and temperature are quantitatively described by Eq. (1) which should serve as an important benchmark for theories of the dynamics of dense fluids. Third, the phenomenon of melting has a negligible effect on the short-time dynamics—in marked contrast to the large discontinuities it causes in static properties. Fourth, the measured scattering efficiencies have confirmed recent theoretical estimates for the solid and provide insight into the mechanisms of nonlinear optical effects in simple condensed media.

We are grateful to Dr. N. R. Werthamer for helpful discussions.

¹See, for example, J. R. Hardy and A. M. Karo, in *Light Scattering Spectra of Solids*, edited by G. B. Wright (Springer, New York, 1969), p. 99; M. Krauzman, *ibid.*, p. 109.

²J. P. McTague, P. A. Fleury, and D. B. DuPre, *Phys. Rev.* **188**, 303 (1969); W. S. Gornall, H. E. Howard-Lock, and B. P. Stoicheff, *Phys. Rev. A* **2**, 1288 (1970); J. A. Bucaro and T. A. Litovitz, *J. Chem. Phys.* **55**, 3585 (1971).

³E. Helfand and S. A. Rice, *J. Chem. Phys.* **32**, 1642 (1960).

⁴N. R. Werthamer, R. L. Gray, and T. R. Koehler, *Phys. Rev. B* **2**, 4199 (1970).

⁵We thank D. Batchelder and R. O. Simmons for helpful advice on the care of rare-gas solids.

⁶Y. Kato and H. Takuma, *J. Opt. Soc. Amer.* **61**, 347 (1971).

⁷P. A. Fleury, J. M. Worlock, and W. B. Daniels, *Phys. Rev. Lett.* **27**, 1493 (1971).

⁸R. E. Slusher and C. M. Surko, *Phys. Rev. Lett.* **27**, 1699 (1971).

⁹N. R. Werthamer, private communication; Werthamer, Gray, and Koehler, Ref. 4.

¹⁰R. W. Hellwarth, *J. Chem. Phys.* **52**, 2128 (1970), and references cited therein; R. W. Hellwarth, A. Owyong, and N. George, *Phys. Rev. A* **4**, 2342 (1971).

¹¹J. P. McTague, C. H. Lin, T. K. Gustafson, and R. Y. Chiao, *Phys. Lett.* **32A**, 82 (1970).

Harmonic Generation and Parametric Excitation of Waves in a Laser-Created Plasma

J. L. Bobin, M. Decroisette, B. Meyer, and Y. Vitel

Commissariat à l'Energie Atomique, Centre d'Etudes de Limeil, 94-Villeneuve-Saint-Georges, France

(Received 30 January 1973)

We observed the light emitted along a direction 45° from the beam axis when a Nd-glass laser (frequency ω_0) was focused on a solid target. Quite intense lines were found with frequencies $2\omega_0$, $\frac{3}{2}\omega_0$, $\frac{1}{2}\omega_0$. The lines at $2\omega_0$ and $\frac{3}{2}\omega_0$ are broadened on the low-frequency side only. Their occurrence and broadening may be related to parametric excitation of waves.

Parametric excitation of ion acoustic and Langmuir waves, already observed with microwaves,^{1,2} has been suspected to play an important role in the high-flux interaction of laser light with matter.³ On the other hand, harmonic generation in a plasma has been evidenced either with microwaves in the presence of a magnetic field^{4,5} or with laser light.⁶ The former effect was due to the vicinity of a hybrid resonance whereas the latter was attributed to nonlinear electron conduction.⁷

Observation of the coupling between the two mechanisms will be reported here, the driving frequency being in the optical range.

The experimental arrangement is sketched in Fig. 1. It was partially described in another paper.⁸ Spectral observations were made using a Czerny-Turner grating spectrometer with a mean

dispersion of 8 \AA/mm in the first order. For recording in the visible range we used a multichan-

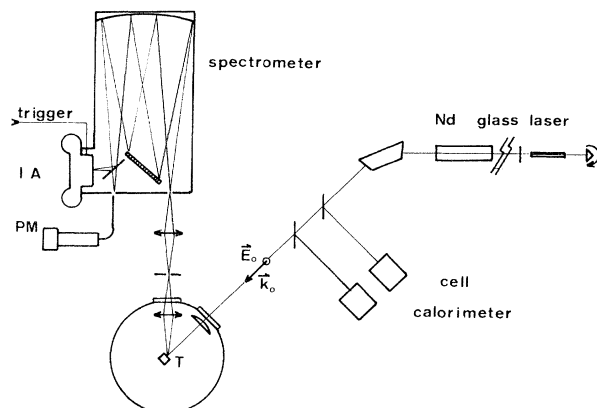


FIG. 1. Experimental setup.